LOW VELOCITY IMPACT OF COMPOSITE CROP STRAW PANELS

Hemdan Abou-Taleb, Aly Sakr

Textile Engineering Department, Faculty of Engineering, Mansoura University, 35516 Mansoura, Egypt
E-mail: haboutaleb_mm@ yahoo.com

Abstract:

The shock behaviour of crop straw reinforced composites with unsaturated polyester epoxy was studied. In this research an attempt has been made to design and manufacture protective composite vests for soldiers. The low velocity impact loading was generated by a drop weight impact machine with drop heights varying from 100 to 200 mm. The drop mass used in these experiments was 15 kg. The shock-absorbing capacity of the vests was found to be strongly affected by straw type, straw weight percentage per unit volume of composite panel (the permanent composite volume of the panel is equal to 434.2 cm^3), and broken short rounded straight steel wire to straw weight ratio. This research concerns the evaluation of all the low velocity drop weight test parameters such as peak dynamic force, duration time, and impulse due to free falling of drop mass at different impact energies: 1.5, 2.25, and 3 J. In addition, indentation parameters such as contact force and absorbed energy could be evaluated. Mathematical models describing these parameters are presented in a form that can be easily predicted. The predicted shock-absorbing capacity shows good agreement with the experimental results. In addition, the optimum tailoring variables affecting the shock-absorbing performance of the composite vest system could be determined.

Key words:

Drop weight, indentation, peak force, impulse, contact force, regression analysis

1. Introduction

Composite is a material that contains at least two different components, clearly separated one from another and uniformly filling its volume, produced in order to create particular properties.

Natural fibers have been used as reinforcement in composite materials since the beginning of our civilisation, when grass and straw or animal hair was used to reinforce mud bricks, also known as adobe [1]. In ancient Egypt, some 3000 years ago, pharaoh mummies were wrapped in linen cloth impregnated with Dead Sea salts, natural resins, and honey in order to protect and reinforce them. These were, most likely, the first known man-made material composites in human history [2]. To improve the properties of materials, man imitated patterns occurring in nature.

Moreover, the possibilities for applications of natural vegetable fibres (NVF) for technical purposes are increasing. Also of importance is the fact that recycling natural fibre reinforced composites (NFRCs) is simpler and the amount of waste is lower. An increase in the production of natural fibre–containing composites also creates economic opportunities in agriculture and rural areas in particular.

The mechanical properties of vegetable fibres are very good and may successfully compete with glass fibre in terms of strength and strength modulus, which is related to the density of fibre. Vegetable fibres show greater elongation when broken than glass or carbon fibres, which may be good for the performance of composites.

The interest in natural fibre reinforced polymer composite materials is rapidly growing both in terms of industrial applications and fundamental research. These fibres are incorporated into matrix materials such as thermosetting plastics, thermoplastics, or rubber. The significant weight savings and the ease and low cost of the raw constituent materials make these composites an attractive alternative to glass and carbon fibre materials.
The combination of a plastic matrix and reinforcing fibres gives rise to composites having the best properties of each component. Since the plastics are soft, flexible, and lightweight compared to other fibres, their combination provides a high strength to weight ratio in the resulting composite.

The properties of composites depend on those of the individual components and on their interfacial compatibility.

The stress transfer at the interface to different phases is determined by the degree of adhesion [3, 4].

In order to achieve improved fibre-matrix bond characteristics and to enhance fibre dispensability in the composite mix, straight steel fibres (wire segments) are produced by cutting or chopping wire typically having a diameter between 0.25 and 1.0 mm, a length ranging from 19 to 60 mm, and an aspect ratio (length/diameter) ranging from 30 to 100. The ultimate tensile strength of steel fibre ranges from 345 to 1700 MPa and the Young's modulus is 205 MPa [5–9].

As long as the aspect ratio of the fibre is less than 50, the fibres may be dispensed directly without any risk of balling. With higher aspect ratios some manufacturers employ special packing techniques to reduce the risk. However, visual inspection during pouring is necessary to check that fibre distribution is satisfactory .

Impact strength and toughness, defined as energy absorbed to failure, are greatly increased; the increase in toughness

results from the increases in tension and flexure of the area under the load deflection curve. Increased resistance to dynamic load and fatigue is often claimed; it seems to be related to the distribution of the fibres in the composite.

The addition of reinforcing fibres is at a recommended dosage of approximately 0.9 kg/m^3 (0.1% by volume), a fibre volume so low that mixing techniques require little or no modification from normal practice. The fibres may be added at either a conventional batching/mixing plant or by hand to the ready mix truck on site. Reinforcing fibres impart a cohesive effect by holding epoxy at or near the surface of the composite. The slump of fibre-dosed composite is not significantly affected by the addition of crop straw [10].

The price of polymer composites reinforced with natural fibres is from two to three times lower than that of polymers reinforced with glass fibre. The low density of natural vegetable fibres can be disadvantageous in processing due to the necessity for pressure application (the fibre tends to emerge on the surface).

There is still insufficient knowledge about the best properties to use for composites and the best modification methods. Low velocity impact damage in composites is especially insidious because the surface damage is often minor and difficult to detect, while the internal hidden damage may be extensive. High mass/low velocity impacts are generally simulated by drop weight tests on composite coupons.

The aim of the present work is to study the shock performance of crop straw reinforced composites commingled with short broken steel wire.

2. Experimental Work

2.1. Samples Preparation

The solid waste materials (crop straw) used in this study and obtained from different locations were wheat, rice, and corn straw. Crop straw-mineral composite specimens containing only one of these waste materials were prepared. Three different weight values of crop straw per permanent composite volume with 12 mm thickness (15, 30, and 45 g) were utilised for each reinforced straw. Results for a control reinforced composite specimen (Twaron) were also obtained from the literature to be used as a reference point with which to compare the results for the reinforced composites containing waste materials (crop straw).

The procedure followed to prepare the tested specimens was chosen in accordance with standards for unsaturated polyester base resin at room temperature, and broken short rounded straight steel wire with a density of 7.85 g/cm3 was added at either a conventional batching/mixing plant or by hand to the ready mix truck in the rectangular mould (22 cm × 16 cm). The average density of wheat, rice, and corn straw was 0.6 g/cm3. All the prepared specimens were cured for 2 days to reach the maximum required strength. The procedure followed in making and curing all the tested composite specimens was in accordance with ASTM c192-900 standards.

Two layers of rubber sheet of 2 mm thickness were bonded on both sides of the composite crop straw panel by adhesive synthetic resin.

In this investigation, five shock impact parameters were measured and evaluated.

Six different panels were constructed with various factors; for example, straw type (X1), straw weight, g/434.2 cm^3 (X2), and steel wire/straw weight ratio (X3) in the composite vest system. The characteristics of these panels are listed in Table 1.

Table 1. Characteristics of reinforced composite panels.

Target no.	Straw type (X1)	Straw weight, g/434.2 cm^3 (X2)	Steel wire/ straw weight ratio(X3)	Fibre volume fraction	Panel weight (kg/m^2)	Panel thickness (mm)	Panel density (g/cm^3)
1	Corn	15	6	24.32	11.9	12	0.990
2	Wheat	45	6	42.83	19.9	12	1.655
3	Wheat	15	20	31.06	20.2	12	1.680
4	Rice	30	6	33.64	18.1	12	1.522
5	Rice	15	13	27.23	14.8	12	1.235
6	Wheat	30	13	39.06	21.9	12	1.824

2.2. Mixture Design

We chose the simplex lattice method for the experiments because of its obvious advantage of being able to analyse all the quadratic and interaction effects [11–13].

For binary systems using three components (Q = 3) the regular 2-simplex is an equilateral triangle with its interior. Each point of the triangle corresponds to a certain composition of the ternary system, and conversely each composition is represented by one distinct point. In the Bozebum triangle, the composition of a ternary system is read from three segments of one side as shown in Figure 1.

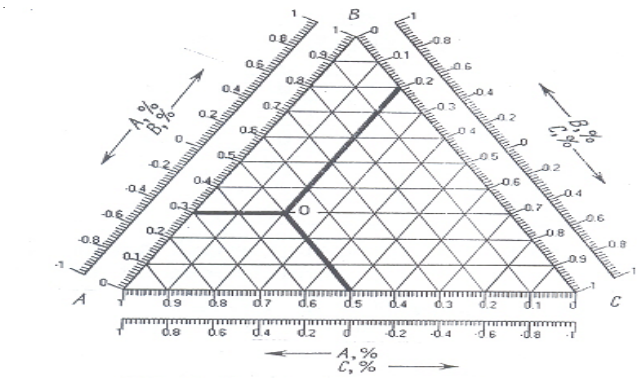

Figure 1. Rozebum´s concentration triangle.

The experiments carried out on composite vest systems were planned according to the simplex lattice method for the three variables, namely straw type (X1), straw weight, g/434.2 cm^3 (X2), and steel wire/straw weight ratio (X3) of the composite vest system.

The range of variation of these factors is given in Table (2). The design of the simplex lattice method for three components is given in Table (3), and the mixture levels of the simplex lattice method are converted to factorial design levels as listed in Table (3).

The second-degree polynomial of mixture design in three components has the general form:

$$Ý = Bi\,Xi + Bij\,Xi\,Xj \qquad (1)$$

Table 2. Range of variation of studied factors.

Factors	Levels			Interval
	–1	0	1	
X1 straw type.	wheat	rice	corn	----
X2 straw weight, g/434.2 cm^3	15	30	45	15
X3 steel wire/straw weight ratio	6	13	20	7

Table 3. Experimental design of studied factors.

Target No.	Coded levels of factors					
	Simplex lattice method			Factorial design method		
	X 1	X2	X3	X 1	X 2	X 3
1	1	0	0	+1	–1	–1
2	0	1	0	–1	+1	–1
3	0	0	1	–1	–1	+1
4	0.5	0.5	0	0	0	–1
5	0.5	0	0.5	0	–1	0
6	0	0.5	0.5	–1	0	0

where:

Ý = the measured response for each experiment,
bi = the coefficient of the main factor effects,
bij = the coefficient of the interaction effects, and
q = the number of factors chosen.

In order to determine the regression coefficients, the response (Ý) has to be found by using different experimental combinations of the variables under consideration.

The mathematical models obtained by the simplex lattice method can be modified by converting the coded levels of factors (0, 0.5, 1) to correspond with the factorial design levels (–1, 0, +1), as listed in Table 3.

2.3. Low velocity drop weight impact test

In order to obtain low velocity and high mass impact conditions, a drop weight tower was used for the impact test.

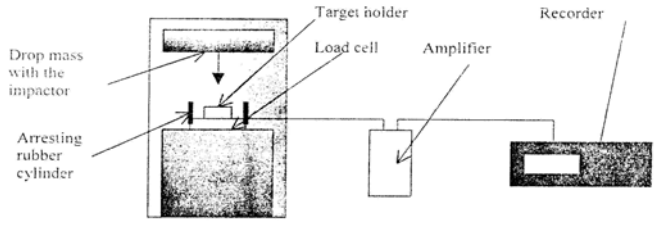

(a) Schematic layout of low velocity dynamic test

(b) Photograph showing method of testing the vest

Figure 2. Drop weight tower impact testing configurations.

In this study, an instrument drop weight impact tower with impactors of different shapes was designed and built. An illustration of the drop weight tower is shown in Figure (2).The tower consisted of two vertical steel rods mounted on a heavy steel base. On the steel base was a fixture suitable for a clamped end and simple support configurations. Attached to the steel rod was a fixed squared crossbar of a hollow steel box beam. An instrumented hardened steel cylindrical impactor joined with a vertical squared rod was attached to the bottom side of the cross-bar by a sliding bearing Figure 2.

Target specimens were cut from the supplied material into 160 x 220 mm rectangular plates and secured into a target holder by clamping at the top and bottom of the specimen. The test specimens had an exposed circular shape of 120 mm diameter and were fixed in the target holder by means of six bolts equally spaced around the circumference at the corners.

The total weight of the impactor with the cylindrical head was 15 kg. It was allowed to fall freely with an impactor diameter of 4 cm, and a range of drop heights varying from 0.1 to 0.2 m was utilised. Incident impact energies in the range of 1.5 to 3.0 J were achieved by varying the drop height. The impact velocity ranged from 0.45 m/sec to 0.63 m/sec.

A load cell strain gauge (force transducer) was fastened (mounted) on the lower surface of the target holder and placed at the base of the tower. The impactor with a cylindrical head was dropped from different heights, producing various load levels. The output signal was processed through a charge amplifier and then dispatched to a transient recorder (digital oscilloscope). For each drop, responses from the strain gauge were recorded and installed on a PC. Impulse due to free falling of the drop weight mass is not sufficient to describe the shock-absorbing performance, so more parameters are required to explain the shock performance of composite crash vests.

The signal of impact force was measured by a force transducer (strain gauge) whose sensitivity was 219.2 mv/kN and then transferred to an oscilloscope via a model KFG-5-120-C1-11 power transducer.

2.4. Static indentation test

Compression after impact (CAI) tests were performed on damage laminates, following ASTM D7137 [14].

The purpose of the indentation test was to establish the static-force-indentation relation between the impactor and the panel. A similar procedure was used by Sabita and Sahay [15] for composite plates.

Finally, CAI tests were performed in a model 5500 R Instron Tester according to [14], as shown in Figure 3.

The dimensions of the specimens were 160 mm x 220 mm. Spherical steel indentors with a diameter of 14 mm were used in the test. The panel specimen was tested on a thick

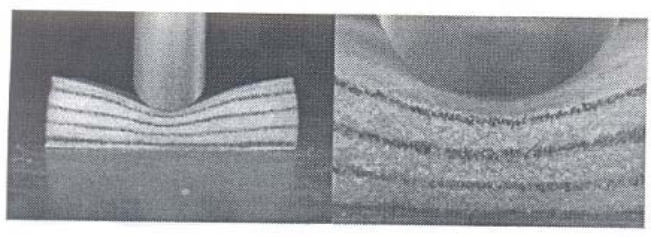

Figure 3. Indentation in composite panel.

steel block, and an Instron Tester was used at a given displacement rate of 10 mm/min to drive the indentor into the specimen in stroke-control mode. The stroke output yielded the amount of indentation. At different stages of loading, the stroke was reversed and unloading curves were obtained.

3. Results and discussion

3.1. Shock impact parameters

Composite panels are often subjected to impacts that do not penetrate or cause visible damage and yet may cause internal damage. With these materials, maximum load is less important than the load and energy at the onset of damage.

The force histories show multiple oscillations before peak load for all samples at all energy levels, which may result from vibrations of the supports and the initiation of damage to the material.

As illustrated in Figures (4–9), the resultant peak forces of panels S3 and S6 were greater than those of S1, S2, S4, and S5. This difference can be explained by the fact that the greater the orientation difference between the panels, the greater the damage caused by the impact loading. Therefore for panels S3 and S6, less damage was caused compared to S1, S2, S4, and S5.

From Figures (4–9), the maximum peak force, duration time, and absorbed energy (impulse) values are extracted and listed in Tables (4–6).

In this section the results of low velocity drop weight tests on six types of new construction are listed in Tables (4–6) and discussed; for this study the aramid Twaron is selected as the control textile material for comparison purposes. For the purpose of comparison each target impulse is normalised according to Twaron and is shown in Figures (10–12).

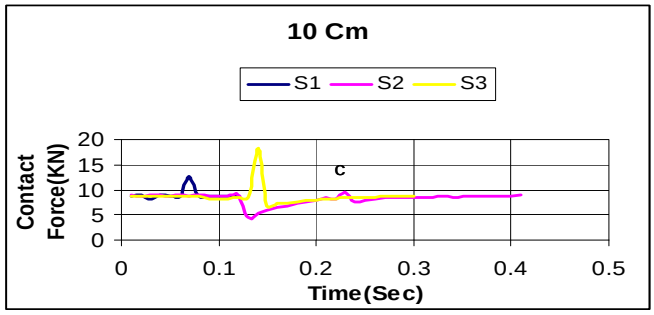

Figure 4. Force–Time History for 1.5 J.

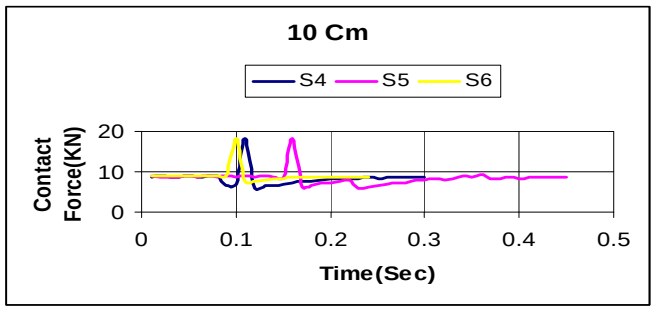

Figure 5. Force–Time History for 1.5 J.

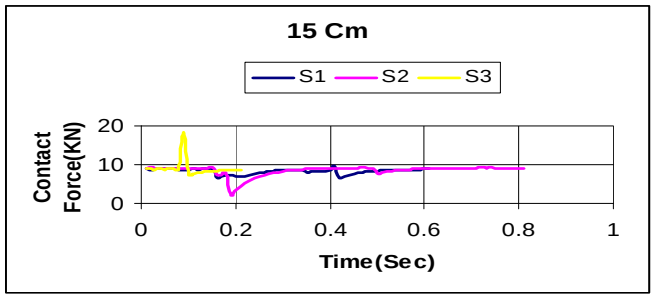

Figure 6. Force–Time History for 2.25 J.

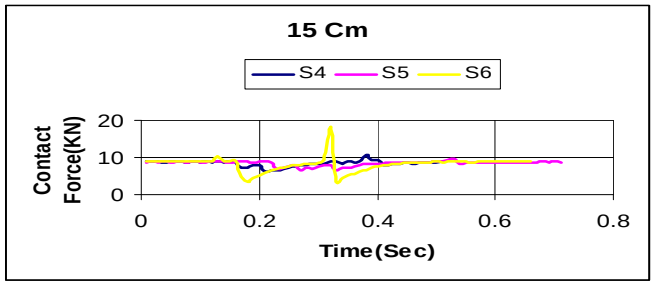

Figure 7. Force–Time History for 2.25 J.

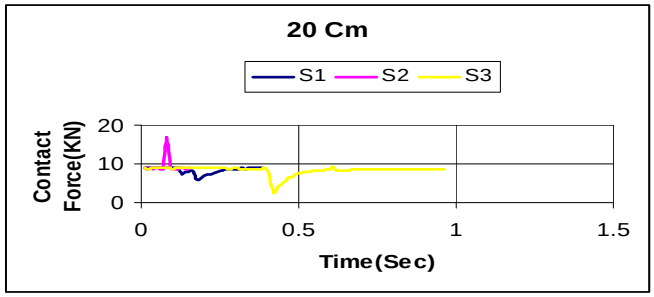

Figure 8. Force–Time History for 3 J.

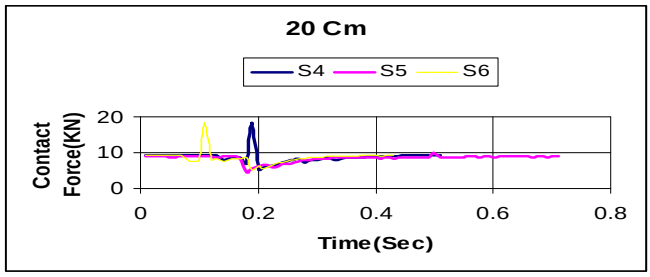

Figure 9. Force–Time History for 3 J.

At Drop Height (10 cm = 1.5 J)

Target type S31 exhibits the largest force, 8105 N, and duration, 0.11 sec, followed by targets S61 and S51, although these have smaller durations. The durations of the remaining targets take values from 23 msec to 232 msec, and the maximum peak force of any one of them is less than that of the above mentioned targets, S31, S61, and F51. The impulse provided by the target in arresting the drop mass is calculated from the area under each curve. These calculations are shown in Figure (10).

From Table (4), it is observed that all six types have impulses larger than that of Twaron, and the increase in the impulse ranges from 81% to 600%. The best target, based on the

impulse generation, is identified as S51, followed by S41 and S21. From Table (4) the targets S51, and S41 generate high impulses. S11 generates an impulse lower than expected, 45.5 N.sec, and this is attributed to its construction.

Table 4. Low velocity dynamic test results at drop height (10 cm = 1.5 J).

Target no.	Peak dynamic force (N)	Duration (msec)	Impulse due to free falling of drop mass (N.msec)	Normalised impulse to Twaron
S11	4000	22.73	45516.6	81.338
S21	3500	270.59	273558.42	488.846
S31	8105	109.09	161718.806	288.990
S41	6421	231.8	298495.4	533.409
S51	6737	19	353193.5	631.154
S61	7789	128	174411.64	311.672
Twaron	370	2.60	559.6	1

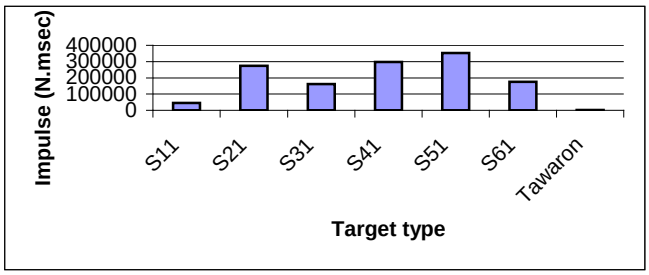

Figure 10. Impulse via different composite panel types (at 1.5 J).

At Drop Height (15 cm = 2.25 J)

Target S32 type exhibits the largest force, 8421 N, and duration, 0.1 sec, followed by targets S22 and S62, although these have smaller durations. The durations of the remaining targets take values from 0.3 sec to 0.45 sec, and the maximum peak force of each of them is less than those of the above mentioned targets, S32, S22, and S62. The impulse provided by the target in arresting the drop mass is calculated from the area under each curve. These calculations are shown in Figure 11.

From Table (5), it is observed that all the types have impulses larger than Twaron, and the increase in impulse ranges from

Table 5. Low velocity dynamic test results at drop height (15 cm = 2.25 J).

Target no.	Peak dynamic Force (N)	Duration time (msec)	Impulse due to free falling of drop mass (N.msec)	Normalised impulse to Twaron
S12	1375	454.55	357299	638
S22	7368	282.35	467481	835
S32	8421	101.6	143137	256
S42	688	311.54	303168	542
S52	2250	305.26	293529	525
S62	3368	340.9	781438	1396
Twaron	370	2.60	559.6	1

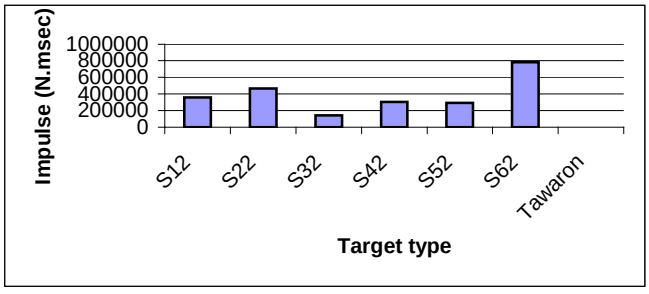

Figure 11. Impulse via different composite panel types at 2.25 J.

250% to 1400%. The best target, based on the impulse generation, is identified as S62, followed by S22 and S12. From Table (5) it is seen that the targets S62, S22, and S12 generate high impulses. S32 generates an impulse lower than expected,143 N.sec, and this is attributed to its construction.

At Drop Height (20 cm = 3 J)

Target type S23 exhibits the largest force, 8095 N, and duration, 0.04 sec, followed by targets S33, S43, and S63 although these have smaller durations. The durations of the remaining targets take values from 0.2 sec to 0.4 sec, and the maximum peak force of each of them is less than those of the above mentioned targets, S33, S43, and S31.

The impulse provided by the target in arresting the drop mass is calculated from the area under each curve; these calculations shown in Figure 12.

From Table 6, it is observed that all the types have impulses larger than Twaron, and the increase in impulse ranges from 163% to 1150%. The best target, based on the impulse generation, is identified as being S43, followed by S63 and S33. From Table 6, it is seen that the targets S43 and S63 generate high impulses. S32 generates an impulse lower than expected, 91.1 N.sec, which is attributed to its construction.

Table 6. Low velocity dynamic test results at drop height (20 cm = 3 J).

Target no.	Peak dynamic force (N)	Duration time (msec)	Impulse due to free falling of drop mass (N.msec)	Normalised impulse to Twaron
S13	3053	245	256510	458
S23	8095	41	91142	163
S33	6158	400	462017	826
S43	4632	440	644546	1152
S53	4313	200	288367	515
S63	4632	330	517991	926
Twaron	370	2.60	559.6	1

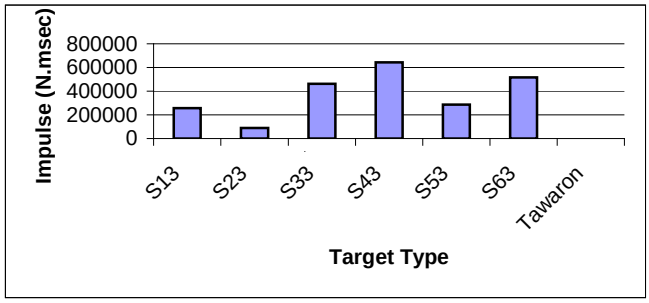

Figure 12. Impulse via different composite panels types at 3 J.

Table 7. Response-surface equations for the composite vest system at 1.5 J.

Response-Surface Equation	R
Y_1 (Peak force, N) = 13144.5 + 5355.5 X_1 + 6407.5 X_2+ 6723.5 X_3 +2671X_1X_2+ 684.5 X_1X_3 + 1986.5 X_2X_3	1
Y_2 (Impulse, N.sec) = 595.6 + 421.2 X_1 + 232.5 X_2 + 297.1 X_3 + 139X_1X_2+ 259.5 X_1X_3 – 43.3 X_2X_3	1

3.1.1. Experimental analysis

As shown in the experimental plan in Table (3) the results obtained for composite vest systems presented in Tables (4–6) were entered into an IBM computer, and the regression coefficients were determined. The response-surface equations for the shock-absorbing parameters are given in Tables (7–9).

Table 8. Response-surface equations for the composite vest system at 2.25 J.

Response-Surface Equation	R
Y_1 (Peak force, N) = 3911.5+ 543.5X_1 –4526 X_2 - 2964 X_3 –3683.5 X_1X_2 –2648X_1X_3 – 4526.5 X_2X_3	1
Y_2 (Impulse, N.sec) = 894.3+112.9X_1 + 600.7X_2 + 591X_3 – 109.2X_1X_2+ 43.3 X_1X_3 – 476.1 X_2X_3	1

Table 9. Response-surface equations for the composite vest system at 3 J.

Response-Surface Equation	R
Y_1 (Peak Force, N) = 4924 + 292.2X_1 + 611 X_2 + 292.2 X_3 – 942 X_1X_2 + 292.5X_1X_3 – 2494.5 X_2X_3	1
Y_2 (Impulse, N.sec) = 1046.1+528.1X_1 + 757.7X_2 + 401.6X_3 + 470.7X_1X_2+ 70.9X_1X_3 – 241.5 X_2X_3	1

The response surface agrees fairly well with the experimental data, as can be seen from the high correlation coefficients. Contour maps were constructed by using the response-surface equations. To understand this interaction, the graphical representation shown in Figures (13–15) was used.

In Tables 10–12 a comparison is shown between measured and calculated values obtained from the response–surface equation with the correlation coefficients between them. The response surface agrees fairly with the experimental data as can be seen from the high correlation coefficients.

Table 10. Comparison between measured and calculated values of the shock-absorbing parameters at 1.5 J

Composite panel no.	Y_1 (peak force, N)		Y_2 (impulse, N.sec)	
	meas.	cal.	meas.	cal.
S_1 1	4000	4000	45.5	45.5
S_2 1	3500	3500	273.6	273.6
S_3 1	8105	8105	161.7	161.7
S_4 1	6421	6421	298.5	298.5
S_5 1	6737	6737	353.2	353.2
S_6 1	7789	7789	174.4	174.4

Table 11. Comparison between measured and calculated values of the shock-absorbing parameters at 2.25 J.

Composite panel no.	Y_1 (peak force, N)		Y_2 (impulse, N.sec)	
	meas.	cal.	meas.	cal.
S_1 2	1375	1375	357.3	357.3
S_2 2	7368	7368	467.5	467.5
S_3 2	8421	8421	143.1	143.1
S_4 2	688	688	303.2	303.2
S_5 2	2250	2250	293.5	293.5
S_6 2	3368	3368	781.4	781.4

Table 12. Comparison between measured and calculated values of the shock-absorbing parameters at 3 J.

Composite panel no.	Y_1 (peak force, N)		Y_2 (impulse, N.sec)	
	meas.	cal.	meas.	cal.
S_1 3	3053	3053	256.5	256.5
S_2 3	8095	8095	91.1	91.1
S_3 3	6158	6158	462.0	462.0
S_4 3	4632	4632	644.5	644.5
S_5 3	4314	4314	288.4	288.4
S_6 3	4632	4632	518	518

3.1.2. Graphical solution

Figures (13–15) are contour plots of each parameter where three dimensions represent three variables in a two dimensional space. The plots show how the studied parameters behave within the limitations of the composite vest system.

The problem of improving the shock-absorbing parameters of the composite vest system can be solved by overlaying all the graphs of the response-surfaces together as shown in Figures 13–15. In Figure 13, it is clear that the shaded area at point A achieves all these parameters and according to this, optimum factors can be accurately defined to realise these parameters. In Figure 13, if the value of (Y_1) was greater than or equal to 5800 N and (Y_2) was larger than 295 N.sec then the desired tailoring variables would be found at point (A), where X_1 = –1 (wheat); X_2 = –1 (15 g) and X_3 = +1 (20). Thus, Figure 13 shows one graphical solution which represents all the investigated parameters.

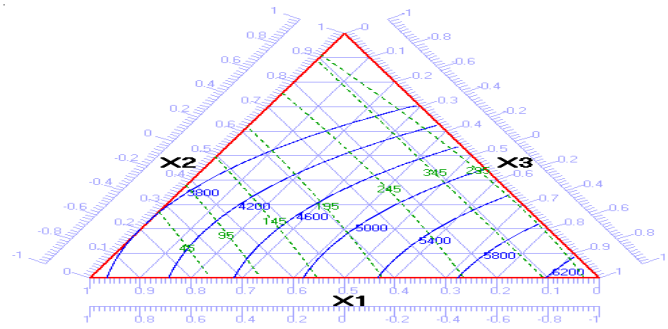

Figure 13. Overlap of peak dynamic force (——) and impulse (——-) contours of straw composite panels at 1.5 J.

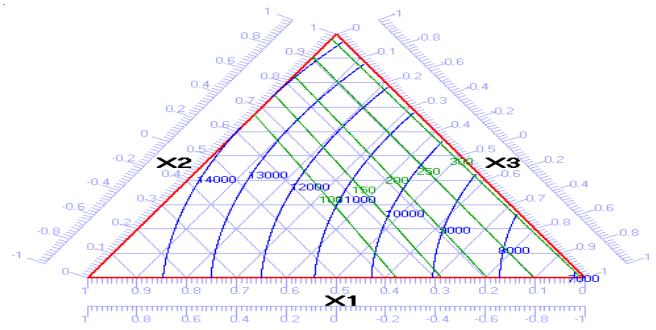

Figure 14. Overlap of peak dynamic force (—) and impulse (—) contours of straw composite panels at 2.25 J.

In Figure 14, if the value of (Y_1) was greater than or equal to 13000 N and (Y_2) was larger than 250 N.sec, then the optimum variables would be found at point (B), where X_1 = –1 (wheat), X_2 = +0.8 (42 g), and X_3 = –0.8 (7.4). Thus, Figure 14 shows one graphical solution which represents all the investigated parameters.

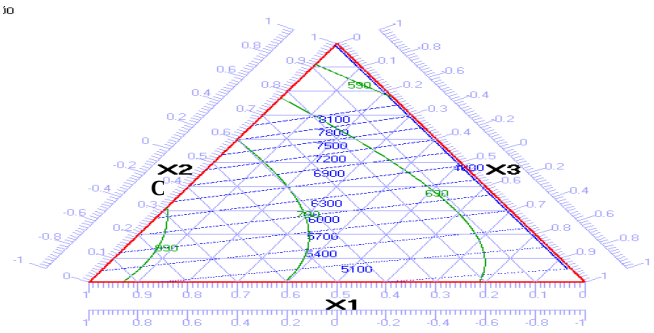

Figure 15. Overlap of peak dynamic force (—) and impulse (—) contours of straw composite panels at 3 J.

In Figure 15, if the value of (Y_1) was equal to 6300 N and (Y_2) was larger than 890 N. sec, then the optimum variables would be found at point (C), where X_1 = +0.4 (60% rice/40% corn), X_2 = –0.4 (24 g), and X_3 = –1 (6). Thus, Figure 15 shows one graphical solution which represents all the investigated parameters.

Generally speaking, the present study was conducted to identify a scientific and practical method to help the manufacturer to select optimum factors according to the required parameters at a low cost.

3.2. Static indentation parameters

The effect of damage on lateral contact loads of a panel was investigated so that the contact loads were introduced without bending effects. A 220 mm × 160 mm × 12 mm straw/epoxy flat panel was statically indented by a steel spherical indentor with a diameter of 14 mm. The typical force-deflection responses from the experiment are shown in Figures (16–21). A new feature in this data is the pronounced softening at very high loads and contact deflection. Presumably this softening is associated with significant damage to the panels, as seen from the depth of penetration and size of the residual "crater" after unloading.

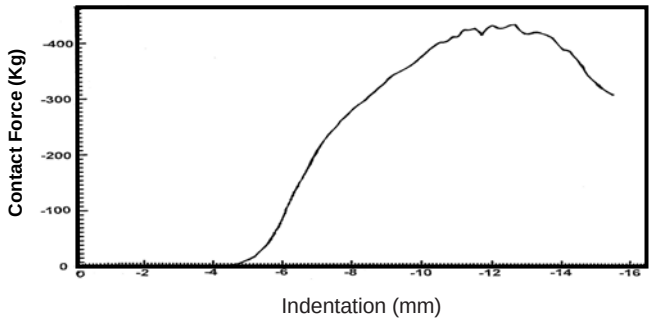

Figure 16. Force-indentation response in contact loading of panel S1.

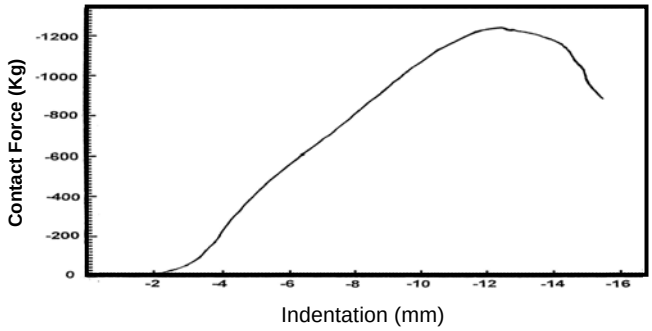

Figure 17. Force–indentation response in contact loading of panel S2.

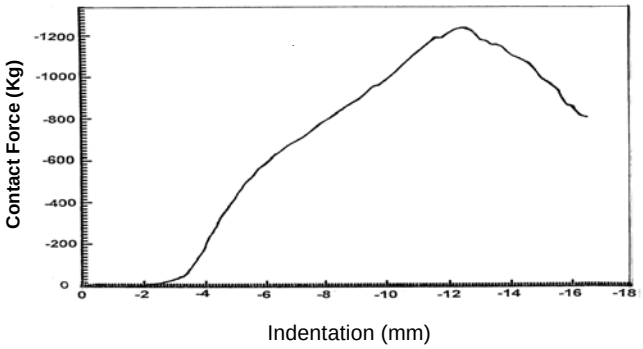

Figure 18. Force–indentation response in contact loading of panel S3.

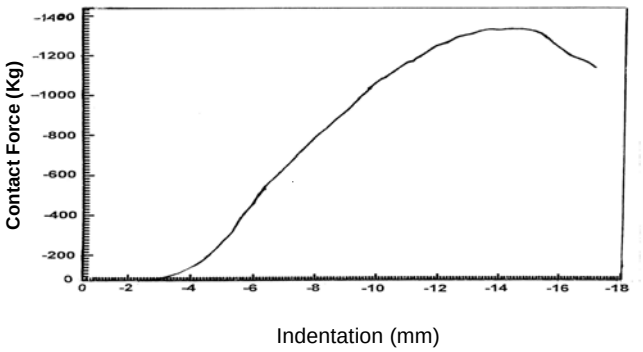

Figure 19. Force–indentation response in contact loading of panel S4.

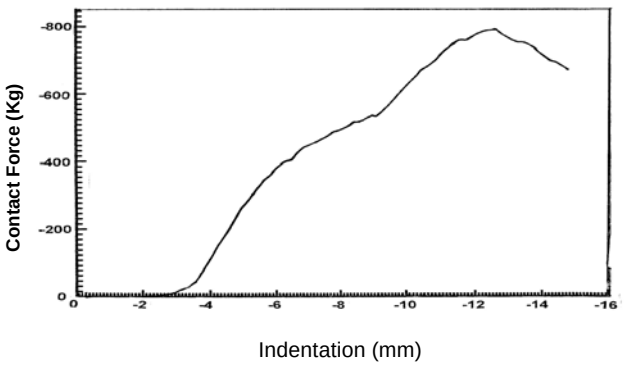

Figure 20. Force–indentation response in contact loading of panel S5.

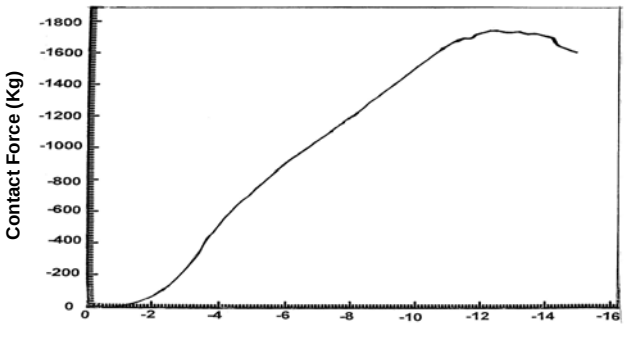

Figure 21. Force–indentation response in contact loading of panel S6.

From Table (13), the targets S3 and S6 generate high absorbed energy. S1 generates an absorbed energy lower than expected, 2225.4 kg.mm, which is attributed to its construction.

Table 13. Indentation test results.

Target no.	Max. contact force (kg)	Indentation (mm)	Absorbed energy (kg.mm)
S_1	433.1	12.6	2225.4
S_2	1236.5	12.4	7053.9
S_3	1238.4	12.5	69894.7
S_4	1259.5	14.0	8456.2
S_5	788.7	12.6	4414.5
S_6	1738.9	12.4	10962.1

3.2.1. Experimental analysis

As listed in the experimental plan in Table (3), the results obtained for composite vest systems in Table (13) were entered into an IBM computer, and the regression coefficients were determined. The response-surface equations for the indentation parameters are given in Table (14).

Table 14. Response-surface equations for composite vest system due to indentation.

Response-Surface Equation	R
Y_1 (Contact force, kg) = $2333.16 + 594.2X_1 + 1544.5\ X_2 + 1073.6\ X_3 + 424.7X_1X_2 - 47.09X_1X_3 + 501.5\ X_2X_3$	1
Y_2 (Absorbed energy, kg.mm) = $12726.8+1764.7X_1 - 20168.7X_2 + 4270.6\ X_3 + 3816.6X_1X_2 - 3164X_1X_3 - 27512.2\ X_2X_3$	1

Figures 22 and 23 are plotted to show the different indentation parameters separately, where each contour line represents a particular value for each parameter. These figures give the manufacturer a wide range of possibilities for choosing the optimum levels of variables to produce a product with the required properties.

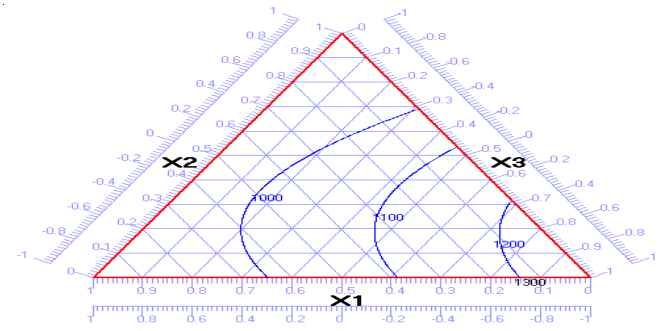

Figure 22. Contact force contours of straw composite panels.

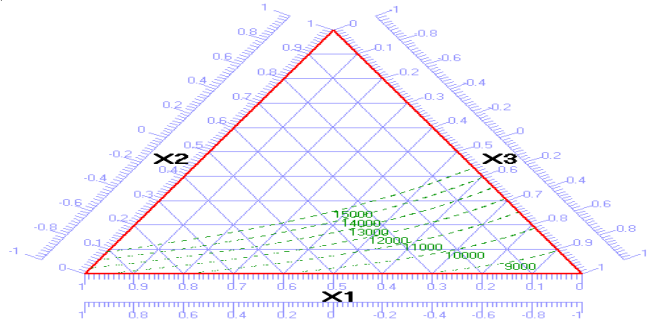

Figure 23. Absorbed energy contours of straw composite panels.

In Table 15 a comparison is given between the measured and calculated values obtained from the response-surface equations with the correlation coefficients between them. The response surface agrees fairly well with the experimental data as can be seen from the high correlation coefficients.

Table 15. Comparison between measured and calculated values of the indentation parameters.

Composite panel no.	Y_1 (contact force, kg)		Y_2 (absorbed energy, kg.mm)	
	meas.	cal.	meas.	cal.
S_1	433.1	433.1	2225.4	2225.4
S_2	1236.5	1236.5	7053.9	7053.9
S_3	1238.4	1238.4	69894.7	69894.7
S_4	1259.5	1259.5	8456.2	8456.2
S_5	788.7	788.7	4414.5	4414.5
S_6	1738.9	1738.9	10962.1	10962.1

3.2.2. Graphical solution

Figures 22 and 23 are contour plots of each parameter where three dimensions represent three variables in a two dimensional space. The plots show how the studied parameters behave within the limitations of the straw composite vest system.

The problem of improving the indentation parameters of the straw composite vest system can be solved by overlaying the graphs (Figures 22 and 23) of the response-surfaces together as shown in Figure 24. In this figure, it is clear that the shaded area achieves all these parameters (contact force and absorbed energy) and according to this, optimum factors can be accurately defined to realise these parameters. In Figure 24, if the value of (Y_1) was equal to 1100 kg or less and (Y_2) was larger than 15000 kg.mm, then the desired tailoring variables would be found at point (D), where X_1 = –0.4 (40% wheat/60% rice); X_2 = –0.4 (24 g) and X_3 = –0.2 (11.6). Thus, Figure 24 shows one graphical solution which represents all the investigated parameters.

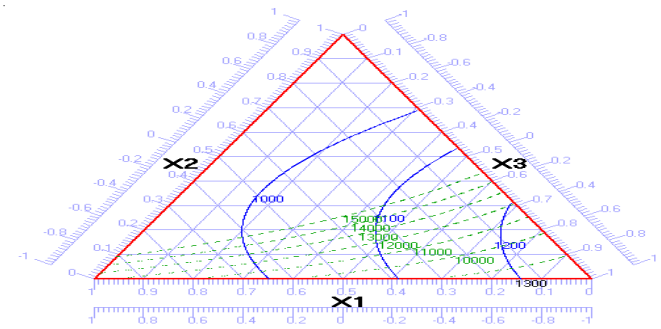

Figure 24. Overlap of contact force (——) and absorbed energy (——-) contours of straw composite panels.

4. Conclusion

From the work described in the research the following conclusions can be drawn.

The optimum construction factors offering the highest shock impact resistance during the drop weight and indentation tests for straw composite panels are:

1. manufacture of composite panels from 20% rice and 80% wheat straw;

2. use of 21 g straw weight per 434.2 cm^3 of the composite panel or 48.4 kg of straw per cubic metre (1 m^3) of composite panel;

3. a ratio of broken short rounded straight steel wire to straw weight in the composite panel of 15.8 using an aspect ratio ranging from 50 to 100.

From observation, it is seen that both the weight and cost of the straw composite panel have the minimum values compared to the Twaron composite panel. Also, both the normalised peak contact force and the impulse or absorbed energy of the straw composite panel have maximum values compared to the Twaron composite panel.

References:

1. *Gook DJ: International fibrous concrete; C 180: 99, 1980.*
2. *Kozlowski R and Wladyka-Przybylak M: Natural fibre reinforced composites. General applications. Chapter (15) in: Natural fibres, polymers and composites: recent advances, FT Wallenberger and PV Kandachar (eds.), Kluwer Academic Publishers, Boston, Dordrecht, London (in press).*
3. *Young RA: Utilization of natural fibres: characterization, modification and applications. In: Lignocellulosic–plastics composites, AL Lea et al. (eds.) Sao Paulo Brazil, 1996.*
4. *Kozlowski R and Przybylak MW: Natural fibers as reinforcing materials for composites. 4th International Conference of Textile Research Division, NRC, Cairo, Egypt, April 15–17, 2007, pp. 272–283.*
5. *ACI Committee 544. IR: Fibre reinforced concrete, American Concrete institute, Michigan, USA, 1990.*
6. *ACIFC: An introduction guide: steel fibre reinforced concrete industrial ground floors, ACIFC, Warwickshire, 1999.*
7. *Knapton J: Ground bearing concrete slabs, Thomas Telford, London, 2003.*
8. *Manolis G, Gareis P, Tsonos A, and Neal J, Dynamic properties of polypropylene fibre-reinforced concrete slabs, Cement and Concrete Composites, 19 (1997) 341–349.*
9. *Newman J and Choo B: Advanced concrete technology (processes), Elsevier Ltd, Oxford, 2003.*
10. *Labib W and Eden N: An investigation into the use of fibres in concrete industrial ground-floor slabs, Liverpool John Moores University, Liverpool.*
11. *Johnson NL and Leone FC: Statistics and experimental design in engineering and the physical sciences, John Wiley, NY, 1977.*
12. *Montgomery DC: Design and analysis of experiments, John Wiley, NY, 1984.*
13. *Akhnagarova S and Kafarov V: Experiment optimization in chemistry and chemical engineering, Mir Publishers, Moscow, 1978 (in Russian).*
14. *D 7137 – Standard test method for compressive residual strength properties of damaged polymer matrix composite plates, Annual book of ASTM Standards International, West Conshohocken, PA, 2005.*
15 *Sabita G, Sahay SK, and Goutam D: Journal of Metallurgical Materials, Science 46/2 (2004), 95.*

Acknowledgements

This research was financially supported by a grant from the Researches Unit of Mansoura University, Egypt.

∇Δ